

ORIGINAL ARTICLE**Asymmetric and symmetric modified bow-tie slotted circular patch antennas for circular polarization**Naresh K. Darimireddy¹  | R. Ramana Reddy² | A. Mallikarjuna Prasad³¹Lendi Institute of Engineering and Technology, Jonnada, Vizianagaram, India.²Department of Electronics & Communications Engineering, Maharaj Vijayaram Gajapati Raju College of Engineering, Vizianagaram, India.³University College of Engineering Kakinada (A), Jawaharlal Nehru Technological University, Kakinada, India.**Correspondence**

Naresh K. Lendi Institute of Engineering and Technology, Jonnada, Vizianagaram, India.

Email: yojitnaresh@gmail.com, yosuna@iecc.org

Modern communication systems employ wideband antennas with circular polarization (CP) radiation. In this work, asymmetric modified bow-tie (ABT) and symmetric modified bow-tie (SBT) slotted circularly polarized single-point probe-fed circular patch antennas with dimensions of 40 mm × 40 mm for wideband applications are proposed. A 10 dB RL bandwidth of 350 MHz with CP, 3 dB axial ratio (AR) bandwidth of 100 MHz, peak gain of 4.9 dBic, and 10 dB RL bandwidth of 530 MHz with CP, 3 dB AR bandwidth of 140 MHz, peak gain of 5 dBic are obtained for ABT and SBT slotted circular patch antennas, respectively. The proposed SBT slotted patch is scaled up and down to 50 mm × 50 mm and 30 mm × 30 mm, respectively. The proposed scaled-up version offers 10 dB RL and 3 dB AR bandwidths of 340 MHz and 80 MHz, with a peak gain of 5 dBic. The scaled-down version offers 10 dB RL and 3 dB AR bandwidths of 710 MHz and 180 MHz, with a peak gain of 5.25 dBic. These prototypes are suitable to work in IEEE 802.11a WLAN, ISM, and IEEE 802.11ac applications. The measured and simulated results are then discussed and compared.

KEYWORDS

AR bandwidth, asymmetric slot, circular polarization, modified bow-tie slot, probe feed, symmetric slot

1 | INTRODUCTION

Small microstrip antennas with circular polarization (CP) radiation and wideband characteristics are required in the era of contemporary wireless communication systems at wireless LAN (WLAN) and WiMAX frequency bands. A reliable transmitter and receiver connection can be offered by CP antennas, as the polarization of the antennas is always aligned. In and around the intended resonant frequency, two modes orthogonal to each other with a phase-shift of 90° is desired for CP. These modes are generated by integration of slots or strips or perturbation on a radiating patch. Single-point feed CP patch antennas [1–3]

occupy smaller areas compared to the dual point feed CP patch antennas and also avoid the need of feed networks. Conversely, the single-point feed CP patch antennas [4,5] commonly have a narrow 3 dB axial ratio (AR) bandwidth and are not appropriate for several wireless applications such as WLAN and ISM bands.

Introducing slits/slots provide compactness to the radiating element. Axial ratio and impedance matching can be optimized by altering the sizes of slits/slots [6]. Embedded V-slit, slot, and stub on circular patch antennas [7] introduce CP with an AR bandwidth of 2.3% in the UMTS frequency band. Compact-size circularly polarized diagonally symmetric slotted microstrip patch (DSSMP) antennas with

different shapes of slots with fixed volume are proposed. Cross-shaped slot DSSMP antenna is compact compared to circular, square, and circular ring-shaped DSSMP antennas. A 3 dB AR bandwidth of 0.7% with 2.0% impedance bandwidth was achieved [8]. Single-feed compact circularly polarized symmetric slit microstrip antennas with different slit shapes along four diagonal directions on the patch are proposed. A measured 10 dB RL bandwidth of 3.85% and 1.5%, and 3 dB AR bandwidth of 1.5% and 0.5% with 0.8 dBic and 3.4 dBic gains were obtained for antennas on the FR4 substrate and the RO4003 substrate, respectively [9]. Compact single coaxial feed microstrip patch antennas with asymmetrical slits in diagonal directions on square patch antennas have been proposed. The measured 10 dB RL and 3 dB AR bandwidths are approximately 2.5% and 0.5%, respectively [10]. A circularly polarized asymmetric circular-shaped patch antenna with slits has been proposed for RFID applications. Without affecting the CP radiation, the operating frequency can be tuned by varying the slit length [11].

Wideband CP radiation can be obtained by probe-fed radiators with truncated corners, symmetric/asymmetric slits/slots, and aperture-coupled radiators with different types of notches or stubs. A circular patch loaded with two shorted balanced pins that offers nearly twice the bandwidth compared to the conventional patch antenna has been presented [12]. The ON-OFF switch operation of PIN diodes [13] between a pair of L-slots provides a wide bandwidth with either right-handed or left-handed CP. By increasing the effective substrate thickness [14], the impedance bandwidth can be enhanced and with an inverted U-shaped patch, the electrical length of the radiating element can be increased. For WLAN, LTE, and WiMAX applications, a compact monopole antenna with a double U-DMS resonator has been presented [15]. A compact monopole antenna fed by a microstrip line with a square radiating patch and a partial ground plane with a notch has been proposed for wideband applications. The defected microstrip U-shapes and notch improve the wideband impedance and gain [16].

Various configurations, including the asymmetric C-shaped slot [17], asymmetric nature of complimentary slit ring resonator with circular slot [18], prefractal asymmetric boundaries [19], combination of parasitic strip and symmetrical corner V-shaped slits [20], integrated unequal circular elements at the corners of square patch [21], and cross-slot-coupled [22] patch antennas have been presented in the literature for CP radiation. Wideband CP antennas with significant gain are an important requirement in modern transceiver systems used for radar and navigational purposes. Considering this aspect, asymmetric and symmetric modified bow-tie slotted circular patch antennas are proposed in this paper for wide bandwidth applications with CP.

2 | CIRCULAR ASYMMETRIC AND SYMMETRIC SLOTTED PATCH ANTENNAS

The fields of the circular patch antenna (CPA) are defined in terms of the Bessel function unlike the case of the rectangular patch antenna, where the fields are defined in terms of cosine and sine functions. The fringing fields along the boundary of the CPA are accounted by effective radius R_e of the circular patch instead of the patch radius R . The fundamental resonant frequency for the CPA is given in (1) as follows:

$$f_{\text{res}} = \frac{Y_{mn} C}{5.714 R_e \sqrt{\epsilon_{\text{reff}}}} \quad (1)$$

where Y_{mn} is the m th root of the derivative of the Bessel function of order n .

ϵ_{reff} = Effective dielectric constant

R_e = Effective radius of the CPA and is given by

$$R_e = R_c \cdot \sqrt{\left(1 + \frac{2 \cdot t}{R_c \cdot \pi \cdot \epsilon_r} \left[\ln \left(\frac{\pi \cdot R_c}{2 \cdot t} \right) + 1.7726 \right] \right)} \quad (2)$$

where R_c is the radius of the CPA, ϵ_r is the dielectric constant, and t is the thickness of the substrate.

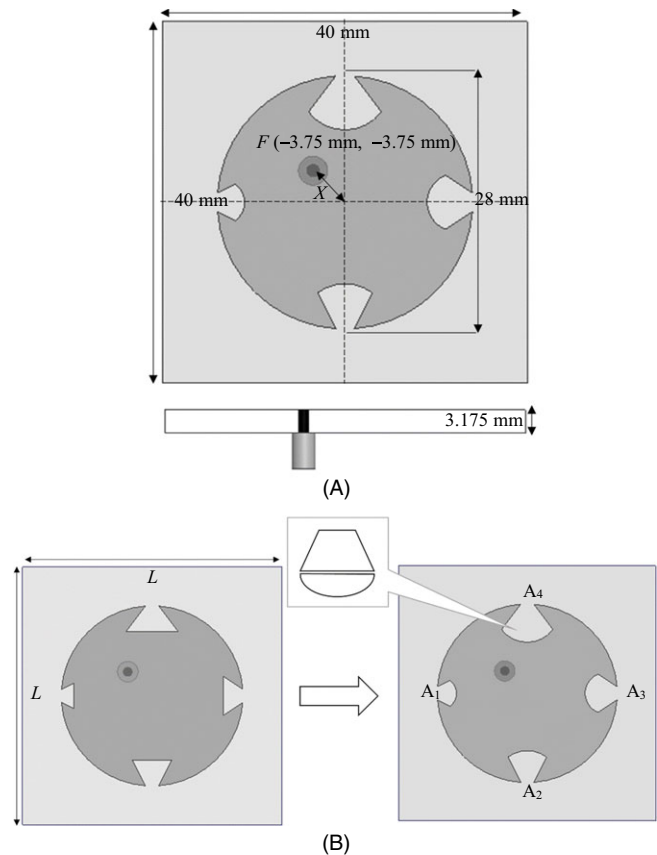


FIGURE 1 (A) Proposed ABT slotted patch antenna and (B) generation of CASP

The effective electrical length of the circular patch can be enhanced by incorporating slots along the circumference. All the four antennas proposed use the modified bow-tie slots for this purpose. The overall size of the proposed antenna is 40 mm × 40 mm, with a circular patch of diameter 28 mm. Low-loss RT/Duroid 5880 with a dielectric constant of 2.2 is used as a substrate with thickness 3.175 mm. Probe feeding is used to feed the signal to the antenna. Asymmetric modified bow-tie (ABT) and symmetric modified bow-tie (SBT) slotted patch antennas are proposed for wideband CP radiation.

3 | CIRCULAR ASYMMETRIC SLOTTED PATCH (CASP)

The proposed ABT slotted patch antenna and its construction with designated dimensions is shown in Figure 1A. The proposed modified bow-tie slot is a combination of a trapezoid and a semiellipse as shown in the inset of Figure 1B. Bow-tie slot areas on the radiating patch are etched according to the relation $A_1 < A_2 < A_3 < A_4$. CP radiation can be achieved by creating asymmetry in the radiating structure with unequal slot areas.

3.1 | Current distributions and CP radiation principle

A pair of modes orthogonal to each other with a phase difference of 90° is produced due to ABT slots etched on the circular patch radiator. The magnitude of surface current

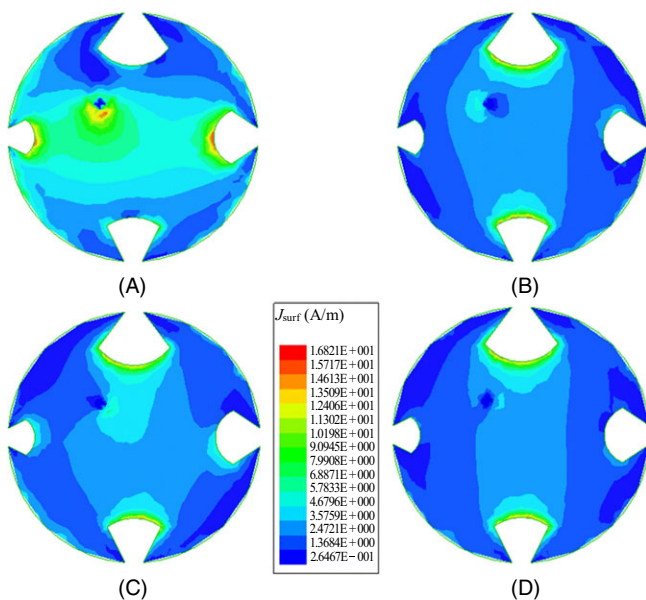


FIGURE 2 Magnitude of surface current densities at different phases: (A) $\theta = 0^\circ$, (B) $\theta = 45^\circ$, (C) $\theta = 90^\circ$, and (D) $\theta = 135^\circ$

densities for the CASP antenna at $Z = 0$ in the XY -plane with respect to four different phases ($\theta = 0^\circ, 45^\circ, 90^\circ$, and 135°) are illustrated in Figures 2A–D. It is evident that the anticlockwise rotation of current densities confirms the left-handed circular polarization (LHCP).

4 | PARAMETRIC STUDY OF CASP

The parametric study is performed to study the performance of the proposed ABT slotted CPA by varying the feed position, and generation of the bow-tie slot from trapezoid and different bow-tie slot areas following the relation $A_1 < A_2 < A_3 < A_4$.

4.1 | Optimization of feed position

The feed is optimized based on the distance between the center of the patch to the feed position, where $F(-3.75 \text{ mm}, -3.75 \text{ mm})$ has a wide bandwidth of 350 MHz, good impedance match, and less return loss compared to all other feed positions as illustrated in Figure 3. RL bandwidths of 310 MHz, 330 MHz, and 340 MHz are obtained for feed positions $F(-3.25 \text{ mm}, -3.25 \text{ mm})$, $F(-3.5 \text{ mm}, -3.5 \text{ mm})$, and $F(-4 \text{ mm}, -4 \text{ mm})$, respectively.

4.2 | Generation of ABT slot

It is evident from Figures 4A and B that the 10 dB RL and AR bandwidths obtained by the trapezoidal slot is 300 MHz (3.04 GHz–3.34 GHz) and 110 MHz (3.05 GHz–3.16 GHz), respectively. Similarly, for the proposed modified bow-tie slot, the 10 dB RL bandwidth is 350 MHz

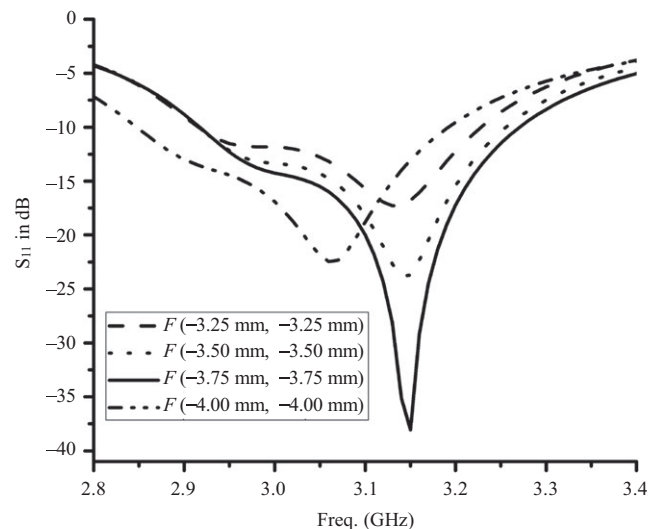


FIGURE 3 S_{11} for different feed positions

(2,910 MHz–3,260 MHz) and the AR bandwidth is 100 MHz (2,950 MHz–3,050 MHz). It is evident from the results that the curvy nature of the bow-tie results in a higher 10 dB RL bandwidth compared to that for the trapezoidal slot.

4.3 | Different Bow-Tie slot areas

Figure 5 shows S_{11} plotted for different bow-tie slot areas, following the inequality $A_1 < A_2 < A_3 < A_4$. The parametric study is conducted for three different slot areas of the proposed ABT slot: $A_1 < A_2 < A_3 < A_4$; X : $A_2 = 2A_1$, $A_3 = 3A_1$, $A_4 = 4A_1$; Y : $A_2 = 2A_1$, $A_3 \cong A_2$, $A_4 = 4A_1$. Among the three slot areas, the proposed ABT slot is having the highest bandwidth of 350 MHz, whereas the X and Y designated ABT slot areas provides 320 MHz and 240 MHz, respectively.

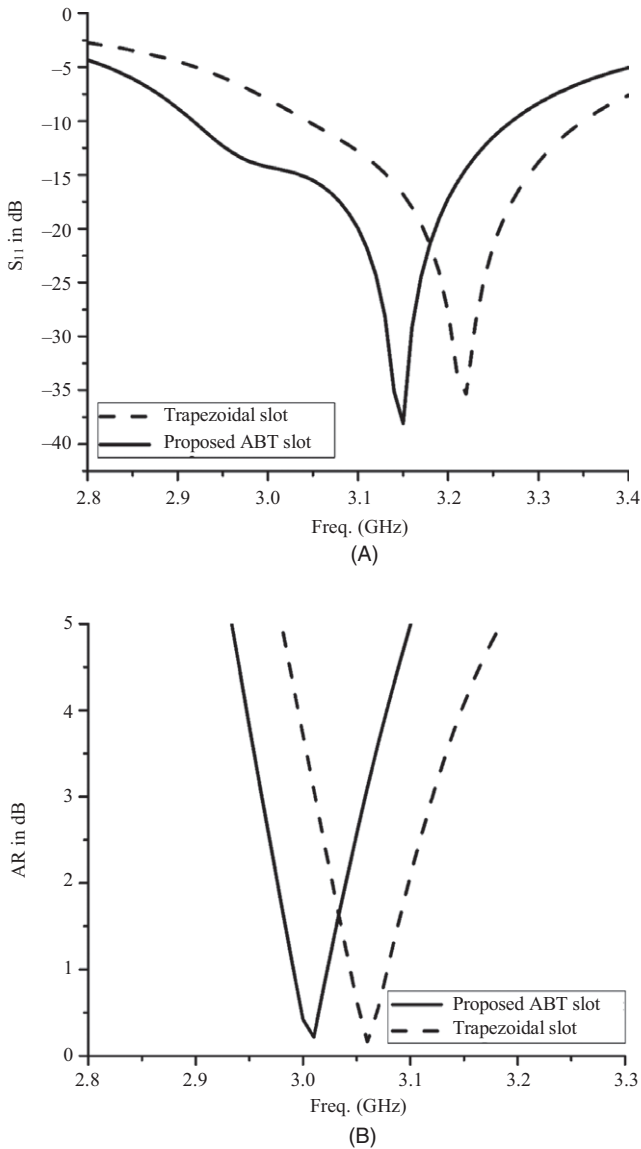


FIGURE 4 (A) S_{11} and (B) AR plot comparison for trapezoidal slot and proposed bow-tie slot

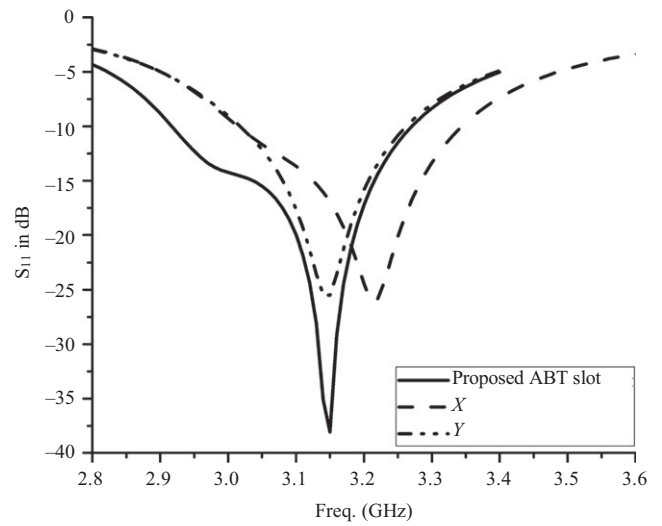


FIGURE 5 S_{11} for different bow-tie slot areas

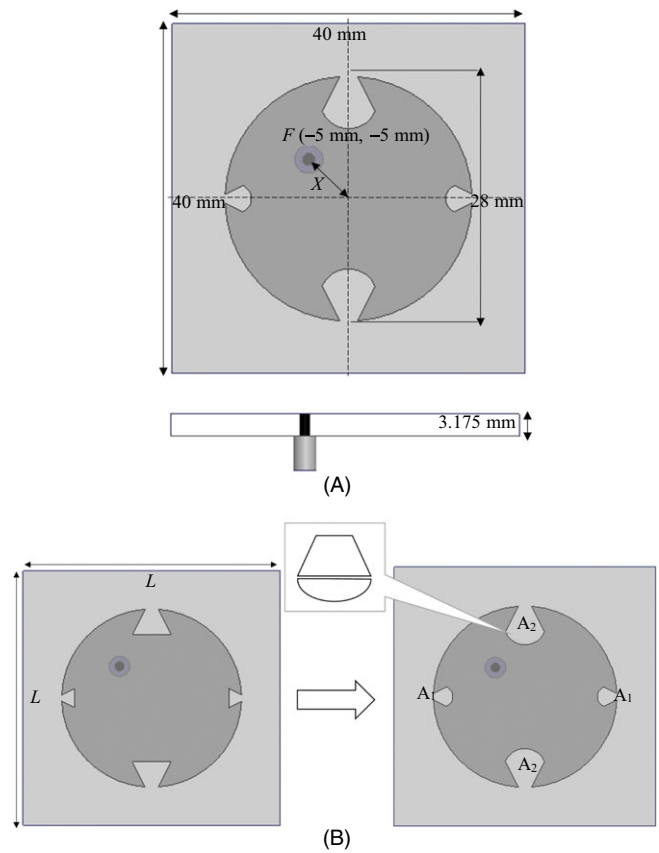


FIGURE 6 (A) Proposed SBT slotted patch antenna and (B) generation of CSSP

5 | CIRCULAR SYMMETRIC SLOTTED PATCH (CSSP)

The construction of the SBT slotted patch antenna with dimensions is presented in Figures 6A and B. The etched

modified bow-tie slots are symmetric with respect to the origin and they are mirror-imaged slot areas ($A_2 = 2A_1$). Comparatively, the SBT slotted patch configuration provides more 10 dB RL bandwidth than the ABT slotted patch with CP radiation.

5.1 | Surface current distributions and CP radiation

By etching symmetric modified bow-tie slotted areas as $A_2 = 2A_1$, two resonant modes orthogonal to each other with a phase difference of 90° are excited and this results in CP radiation. The magnitude of current densities for the proposed SBT slotted antenna at different phases ($\theta = 0^\circ, 45^\circ, 90^\circ$, and 135°) are illustrated in Figures 7A–D. It is evident from the results that the circular motion of current densities is in the anti-clockwise direction resulting in LHCP.

6 | PARAMETRIC STUDY OF CSSP

The performance of the proposed SBT slotted CPA is assessed by the parametric variations such as optimization of feed position from origin, generation of the SBT slot from the trapezoid, and different areas of the modified bow-tie slots following the relation $A_2 = 2A_1$.

6.1 | Optimization of the feed position

S_{11} for different feed positions are presented in Figure 8. From the results, it can be observed that feed point

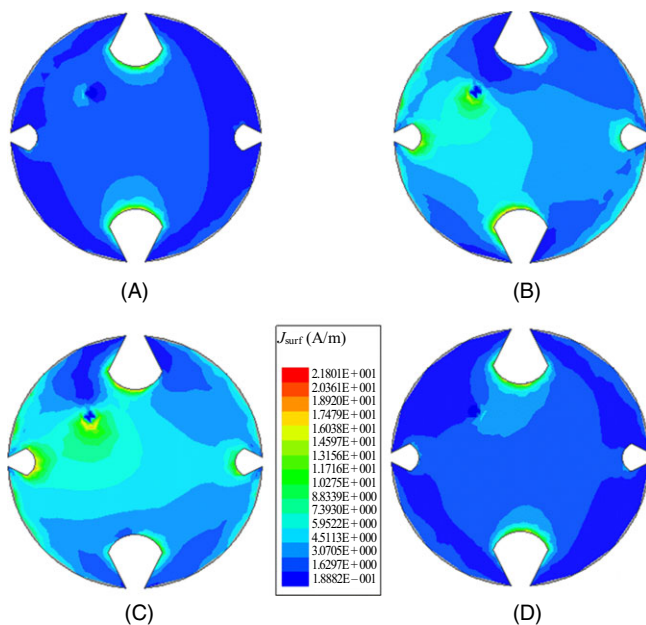


FIGURE 7 Current density distributions at different phases: (A) $\theta = 0^\circ$, (B) $\theta = 45^\circ$, (C) $\theta = 90^\circ$, and (D) $\theta = 135^\circ$

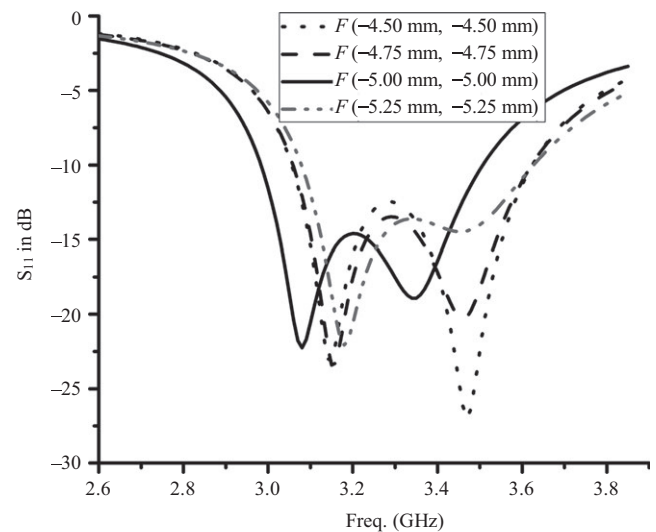


FIGURE 8 S_{11} plot for different feed positions

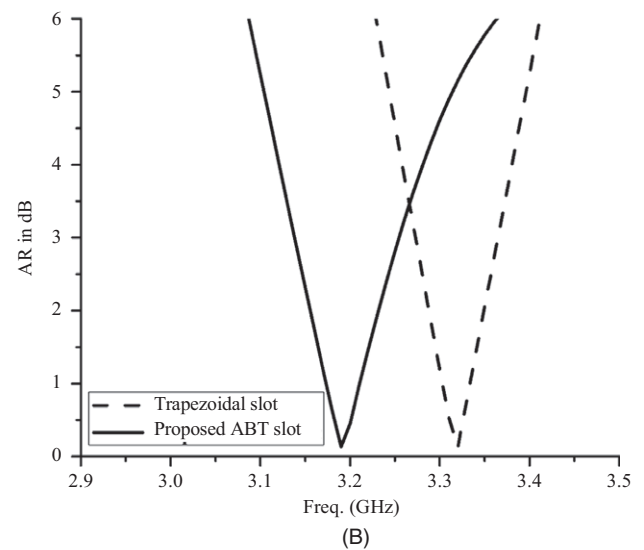
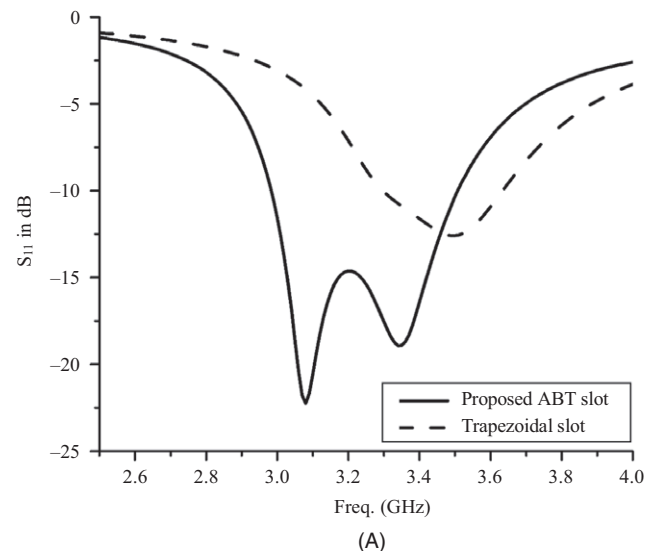


FIGURE 9 (A) S_{11} and (B) AR plot comparison for trapezoidal slot and proposed SBT slot

F (-5 mm, -5 mm) offers good impedance match and maximum radiation. The bandwidth obtained for the proposed feed point is 530 MHz and it is the highest compared to other feed point locations.

6.2 | Generation of SBT slot

From Figures 9A and B, it is observed that the 10 dB RL and AR bandwidths offered by the trapezoidal slot is 350 MHz (3.3 GHz–3.65 GHz) and 120 MHz (3.25 GHz–3.37 GHz), respectively. The proposed SBT slot offers a 10 dB RL bandwidth of 530 MHz (2,980 MHz–3,510 MHz) and an AR bandwidth of 140 MHz (3,090 MHz–3,230 MHz). The curved circumference of the modified bow-tie provides high 10 dB RL and AR bandwidths compared to the trapezoidal slot.

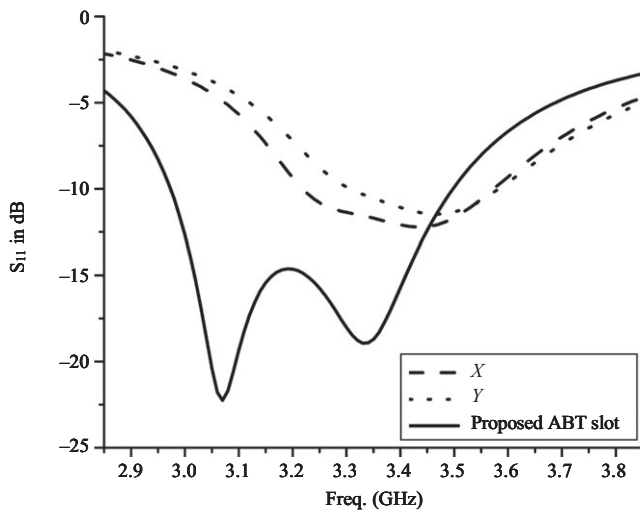


FIGURE 10 S_{11} for different symmetric bow-tie slot areas

6.3 | Different SBT slot areas

Various symmetric modified bow-tie slot areas that are mirror images with respect to the origin are considered for S_{11} as illustrated in Figure 10. The inequality followed for all the areas of the bow-tie slot are $A_2 = 2A_1$, considering $A_1(X) < A_1(Y) <$ proposed area of A_1 .

The final design dimensions were obtained through parametric studies and surface current analysis of the ABT and SBT slotted patch antennas. Similarly, the parametric studies and surface current analysis were also conducted on the scaled-up (50 mm \times 50 mm) and scaled-down (30 mm \times 30 mm) versions of the SBT-CSSP antenna.

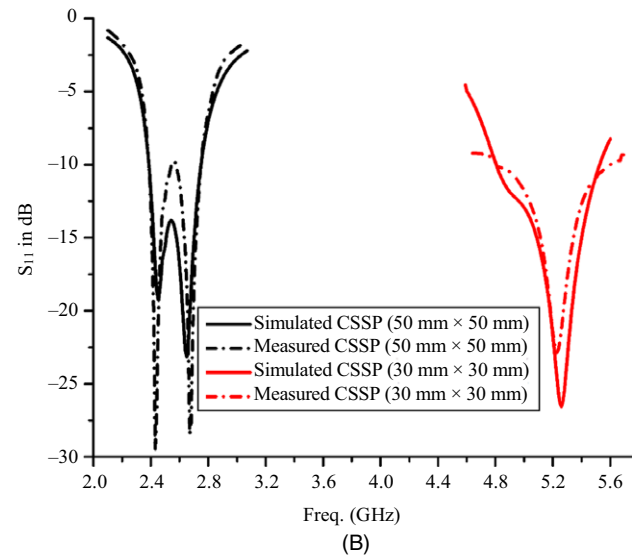
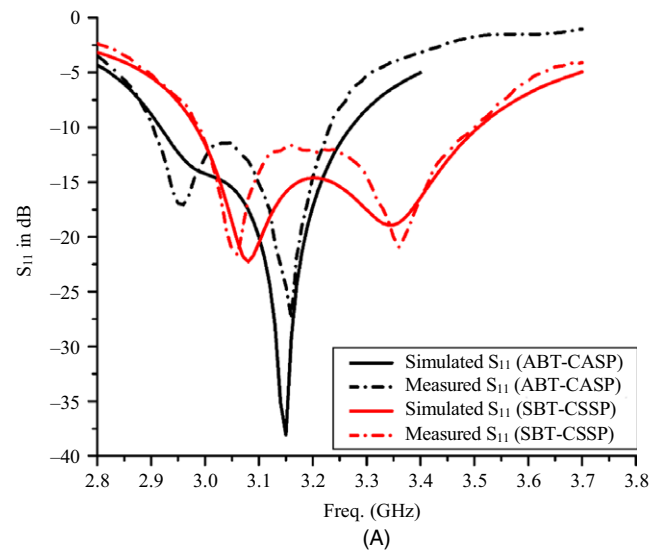


FIGURE 12 Comparison of simulated and measured S_{11} for the proposed antennas: (A) S_{11} for ABT and SBT slotted patches with 40 mm \times 40 mm, and (B) S_{11} for scaled-up (50 mm \times 50 mm) and scaled-down (30 mm \times 30 mm) SBT slotted patches

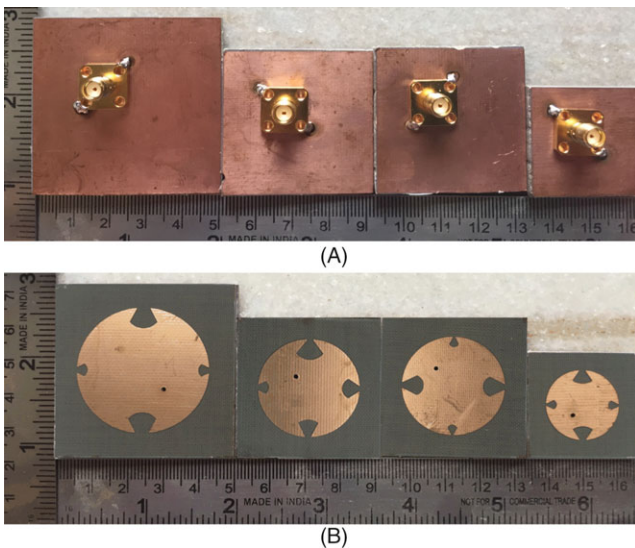


FIGURE 11 Fabricated antenna structures: (A) front view and (B) rear view

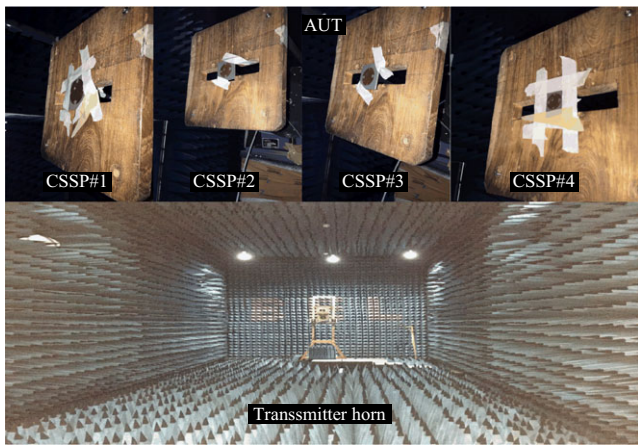


FIGURE 13 Pattern and gain measurement in an anechoic chamber

The proposed scaled-up version offers a 10 dB RL bandwidth of 340 MHz, 3 dB AR bandwidth of 80 MHz, and peak gain of 5 dBic with CP. For the scaled-down version, the 10 dB RL bandwidth of 710 MHz, 3 dB AR bandwidth of 180 MHz, and a peak gain of 5.25 dBic with CP radiation were obtained.

7 | DISCUSSION OF MEASURED RESULTS

All the proposed four antennas fabricated are presented in Figures 11A and B. S_{11} was measured using a vector network analyzer (VNA). Comparison of simulated and measured S_{11} is presented in Figures 12A and B. The radiation pattern, peak gain, and AR were measured in an anechoic chamber, and the setup is shown in Figure 13. The patterns are taken at the CP resonant frequency and the polarization is similar in both the orthogonal planes (XZ and YZ planes) representing CP radiation as shown in Figures 14A–D. The AR and peak gain are measured and the comparison with simulated results is shown in Figures 15A and B. All the proposed four antennas possess wideband CP radiation characteristics with more than 5 dBic gain. It is evident from the results that the simulated and measured results are in close agreement. The small deviations in practical results when compared to simulation results are attributed to fabrication tolerances, and are not considered in the process of simulation.

The performance of the proposed ABT-CASP and SBT-CASP antennas are tabulated and comparison with recent designs is presented in Table 1 in terms of overall size,

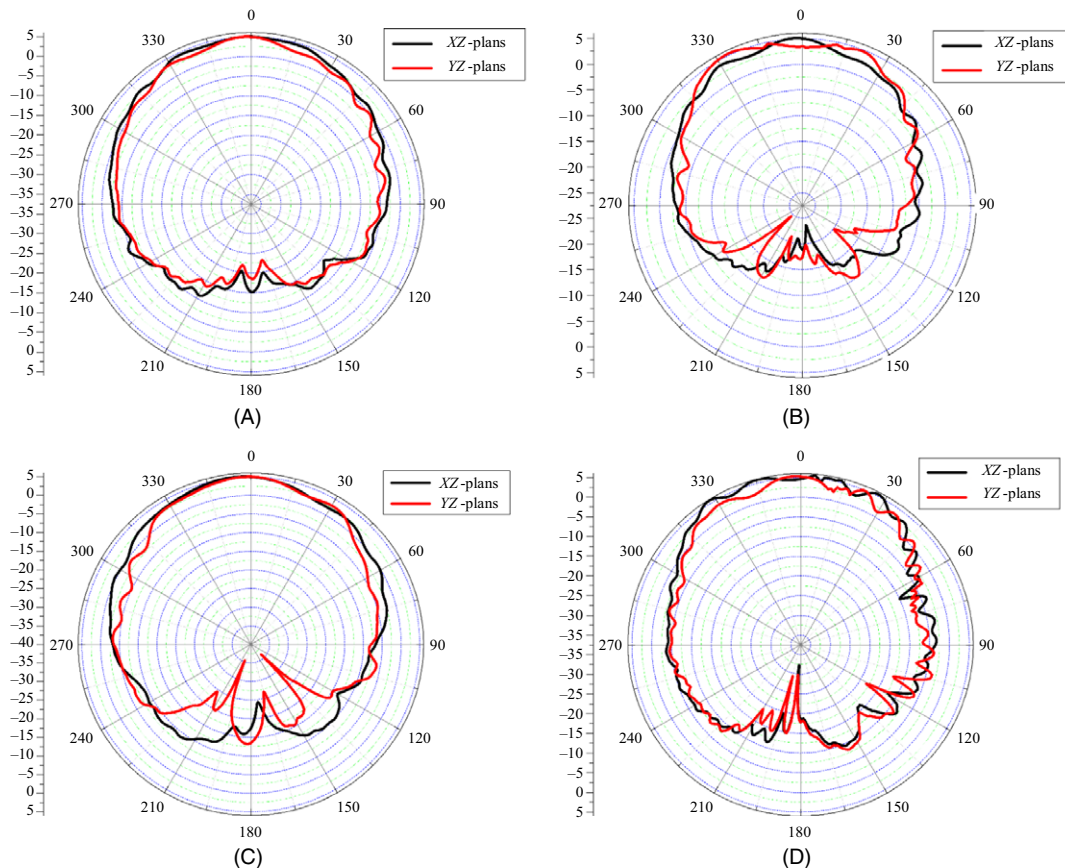


FIGURE 14 Radiation patterns of the proposed antennas in XZ and YZ plane: (A) ABT-CASP at 3 GHz, (B) SBT-CASP at 3.2 GHz, (C) scaled-up CSSP at 2.4 GHz, and (D) scaled-down CSSP at 5 GHz

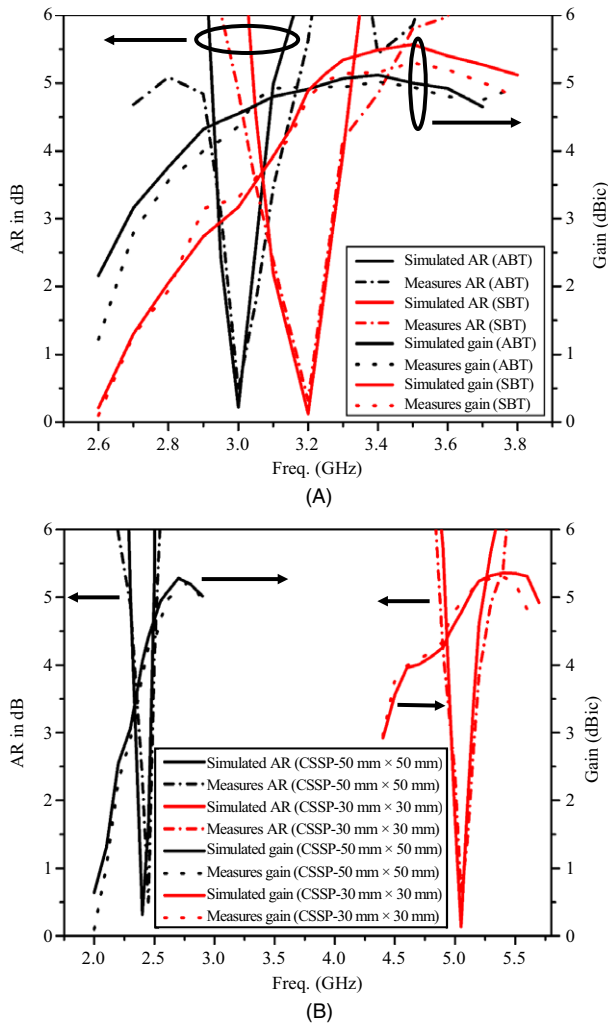


FIGURE 15 Comparison between simulated and measured peak gain along with axial ratio for the proposed antennas: (A) AR and gain for ABY and SBT slotted patch antennas and (B) AR and gain for scaled-up (50 mm × 50 mm) and scaled-down (30 mm × 30 mm) SBT slotted patch antennas

volume (expressed in free-space wave length- λ_0), minimum AR value, 3 dB AR bandwidth, operating frequency range, 10 dB RL bandwidth, and gain. In [18], the radiating patch has a 10 dB RL bandwidth of 552 MHz, but it has a low 3 dB AR bandwidth. Other antennas [19–22] have lower AR and 10 dB RL bandwidths compared to the proposed ABT and SBT slotted patch antennas.

8 | CONCLUSION

ABT and SBT slotted patch antennas (40 mm × 40 mm) were proposed for wideband CP applications. The ABT slotted circular patch offers a 10 dB RL bandwidth of 350 MHz with CP, and a 3 dB AR bandwidth of 100 MHz with a peak gain of 5 dBic. The SBT slotted patch provides a 10 dB RL bandwidth of 530 MHz with CP, and a 3 dB AR bandwidth of 100 MHz with a peak gain of 5.1 dBic. The presented ABT and SBT patches are suitable for S-band applications such as weather radar, surface-ship radar, and communication satellites. The scaled-up SBT-CSSP (50 mm × 50 mm) version possesses a 10 dB RL bandwidth of 340 MHz (2,390 MHz–2,730 MHz) with CP, a 3 dB AR bandwidth of 80 MHz with a gain of 5 dBic; the scaled-down SBT-CSSP (30 mm × 30 mm) version provides a 10 dB RL bandwidth of 710 MHz (4,800 MHz–5,510 MHz) with CP, and a 3 dB AR bandwidth of 180 MHz with a gain of 5.25 dBic. The scaled versions are suitable for IEEE 802.11a WLAN (2.4 GHz), ISM (2.4 GHz–2.485 GHz), and IEEE 802.11ac (5 GHz) applications. Measured and simulation results were in close agreement.

ORCID

Naresh K. Darimireddy  <http://orcid.org/0000-0002-0033-716X>

TABLE 1 Brief introduction to some similar experiments

Ref.	Size (mm ²)	Volume	Min. AR value	3 dB AR BW (MHz)	Operating frequency (MHz)	10 dB RL BW (MHz)	Gain (dBic)
[18]	35 × 40	0.4 λ_0 × 0.457 λ_0 × 0.017 λ_0	1.3	56	3,156–3,708	552	4.43
[19]	42 × 42	0.35 λ_0 × 0.35 λ_0 × 0.027 λ_0	0.42	50	2,455–2,617	162	6
[20]	80 × 80	0.607 λ_0 × 0.607 λ_0 × 0.012 λ_0	1.5	17	2,245–2,307.5	62.5	7.3
[21]	70 × 70	0.373 λ_0 × 0.373 λ_0 × 0.016 λ_0	<0.5	24	1,568–1,592	56	5.25
[22]	50 × 50	0.317 λ_0 × 0.317 λ_0 × 0.048 λ_0	<0.5	28	1,886–1,978	92	4.9
Proposed ABT-CASP	40 × 40	0.39 λ_0 × 0.39 λ_0 × 0.033 λ_0	0.2	100	2,910–3,260	350	5
Proposed SBT-CSSP	40 × 40	0.424 λ_0 × 0.424 λ_0 × 0.034 λ_0	0.12	140	2,980–3,510	530	5.1
Scaled-up SBT-CSSP	50 × 50	0.426 λ_0 × 0.426 λ_0 × 0.027 λ_0	0.3	80	2,390–2,730	340	5
Scaled-down SBT-CSSP	30 × 30	0.515 λ_0 × 0.515 λ_0 × 0.054 λ_0	0.2	180	4,800–5,510	710	5.25

REFERENCES

1. P. C. Sharma and K. C. Gupta, *Analysis and optimized design of single feed circularly polarized microstrip antennas*, IEEE Trans. Antennas Propag. **29** (1983), no. 6, 949–955.
2. M. Haneishi and S. Yoshida, *A design method of circularly polarized rectangular microstrip antenna by one-point feed*, Electron. Commun. Japan (Part I: Commun.) **64** (1981), no. 4, 46–54.
3. K. L. Wong, *Compact and broad band microstrip antenna*, John Wiley & Sons, Inc., New York, USA, 2002, pp. 162–220.
4. H. Iwasaki, *A circularly polarized small size microstrip antennas with cross slot*, IEEE Trans. Antennas Propag. **44** (1996), no. 10, 1399–1401.
5. K. F. Tong and T. P. Wong, *Circularly polarized U-slot antenna*, IEEE Trans. Antennas Propag. **55** (2007), no. 8, 2382–2385.
6. Nasimuddin, *Microstrip antennas*, InTechOpen, London, UK, 2011.
7. S. Mathew et al., *Compact dual polarised V slit, stub and slot embedded circular patch antenna for UMTS/WiMAX/WLAN applications*, IET Electron. Lett. **52** (2016), no. 17, 1425–1426.
8. Nasimuddin, Z. N. Chen and X. Qing, *Slotted microstrip antennas for circular polarization with compact size*, IEEE Antennas Propag. Mag. **55** (2013), no. 2, 124–137.
9. Nasimuddin, X. Qing and Z. N. Chen, *Compact circularly polarized symmetric-slit microstrip antennas*, IEEE Antennas Propag. Mag. **53** (2011), no. 4, 63–75.
10. Nasimuddin, X. Qing and Z. N. Chen, *Compact asymmetric-slit microstrip antennas for circular polarization*, IEEE Trans. Antennas Propag. **59** (2011), no. 1, 285–288.
11. Nasimuddin, Z. N. Chen and X. Qing, *Asymmetric-circular shaped slotted microstrip antennas for circular polarization and RFID applications*, IEEE Trans. Antennas Propag. **58** (2010), no. 12, 3821–3828.
12. D. Guha and Y. M. M. Antar, *Circular microstrip patch loaded with balanced shorting pins for improved bandwidth*, IEEE Antennas Wireless Propag. Lett. **5** (2006), no. 1, 217–219.
13. S. Raghavan, T. Shanmuganatham, and K. Kumar, *Reconfigurable patch antenna with switchable L-shaped slots for circular polarization diversity*, Microw. Opt. Technol. Lett. **50** (2008), no. 9, 2348–2350.
14. T. Shanmuganatham and S. Raghavan, *Design of a compact broadband microstrip patch antenna with probe feeding for wireless applications*, AEU-Int. J. Electron. Commun. **63** (2009), no. 8, 653–659.
15. A. Boutejdar et al., *Compact microstrip antenna covers WLAN, LTE, and WiMAX*, Microw. RF, **50** (2018), no. 1, 13–17.
16. A. Boutejdar, M. A. Salamin, and S. D. Bannani, *Design of compact monopole antenna using double U-DMS resonators for WLAN, LTE, and WiMAX applications*, Telkomnika, **15** (2017), no. 4, 1693–1700.
17. Nasimuddin, Z. N. Chen, *Aperture-coupled asymmetrical c-shaped slot microstrip antenna for circular polarization*, IET Microw., Antennas Propag. **3** (2009), no. 3, 372–378.
18. L. Geng et al., *Compact circularly polarized patch antenna using a composite right/left-handed transmission line unit-cell*, Radio-Eng. J. **22** (2013), no. 1, 286–290.
19. V. Reddy and N. V. S. N. Sarma, *Compact circularly polarized asymmetrical fractal boundary microstrip antenna for wireless applications*, IEEE Antennas Wireless Propag. Lett. **13** (2014), pp. 118–121.
20. M. T. Islam et al., *Compact antenna for small satellite applications*, IEEE Antennas Propag. Mag. **57** (2015), no. 2, 30–36.
21. Nasimuddin, Y. S. Anjani and A. Alphones, *A wide-beam circularly polarized asymmetric-microstrip antenna*, IEEE Trans. Antennas Propag. **63** (2015), no. 8, 3764–3768.
22. J. Li et al., *Miniaturized single-feed cross-aperture coupled circularly polarized microstrip patch antenna*, Progres. Electromag. Res. C **63** (2016), 183–191.

AUTHOR BIOGRAPHIES



Naresh K. Darimireddy obtained his BTech degree in Electrical & Communications Engineering from NBKR Institute of Science and Technology, India ME (EC) from University Visvesvaraya College of Engineering (A), Bangalore University, India, MBA from the Central University, Pondicherry, India, and is presently pursuing his PhD degree from University College of Engineering Kakinada (A), Jawaharlal Nehru Technological University, Kakinada, India. He has 14 years of industry and teaching experience. Darimireddy is a Member of IEEE, IEEE A & P Society, and IE. He is qualified a UGC-NET candidate in 2013, and has 33 technical publications in journals and conferences. His research interests include microwave antennas, filters, and DRAs.



R. Ramana Reddy received his MTech (I&CS) in 2002 from Jawaharlal Nehru Technological University, Kakinada, India MBA from AU in 2007, and PhD degree in Antennas from AUCE (A), AU. He is a Professor and the HOD of ECE in Maharaj Vijayaram Gajapati Raju(MVGR) College of Engineering, Vizianagaram. He is the coordinator of the Center of Excellence in the Embedded Systems and NI LabVIEW academy in MVGRCE. Dr. Reddy has published 90 technical papers in journals and conferences. He is a Senior Member of IEEE, IETE, and ISTE. His research interests include antennas, EMI/EMC, VLSI, and embedded systems.



A. Mallikarjuna Prasad is a Professor of Electronics & Communications Engineering (ECE), and the Vice Principal in University College of Engineering Kakinada (A), Jawaharlal Nehru Technological University (JNTU), Kakinada, India. He obtained his PhD degree from JNTU, Hyderabad, in antennas. Earlier, he was the Head of the Department of ECE and the Controller of Examinations in JNTUK. His research interests include microwave antennas, wireless communications, and biomedical instrumentation.